

Kathleen K. Crahan,^{*} Dean Hegg, David S. Covert and H. Jonsson
University of Washington, Seattle, WA

1. INTRODUCTION

The importance of aerosol forcing in the global radiative budget has been repeatedly recognized by the scientific community, most recently in the current IPCC Climate Change 2001 report. Although the direct forcing of several inorganic compounds, especially sulfates, has been well documented (*Charleston et al*, 1992), the radiative forcing budget of aerosols in general, and of organic aerosols in particular still contain large uncertainties.

One aspect of direct forcing involves the hygroscopicity of aerosols. The chemical composition of the aerosol, as well as the ambient relative humidity, affect how much water condenses upon the aerosol, which in turn affects the light scattering behavior. The phenomenological relationship between RH and particle scattering, σ_{sp} , has been parameterized by the gamma exponent of Kasten (1969) (see also: *Gasso et al*, 2000):

$$\sigma_{sp}(RH) = k(1-RH/100)^{-\gamma} \quad (1)$$

where k and gamma are determined by fitting known data into the equation. In practice k, which in principle is $\sigma_{sp}(RH=0)$ is assumed to be $\sigma_{sp}(RH \leq 40\%)$ and γ alone determines the aerosol hygroscopicity (see *Gasso et al*, 2000).

In principle, one can also determine the aerosol hygroscopicity from the chemical composition of ambient aerosols utilizing theoretical analysis. However, the current unsatisfactory state of solution theory for the complex chemical mixtures which constitute ambient aerosols render this infeasible.

The venue of Project RED (Rough Evaporation Duct) off the eastern shore of Oahu was well suited to study the hygroscopicity and scattering of background marine aerosols. The presumably background nature of the aerosol would suggest that an exploration of the linkage between chemical composition and hygroscopic and optical properties might prove straightforward. However, although relating hygroscopicity to marine salt particles is indeed straightforward, difficulties arise when taking into account the poorly specified organic component of marine aerosols. The fatty acids that are found in marine phytoplankton accumulate on the ocean's surface upon the death and decomposition of the organism, and are likely ejected into the atmosphere along with the salt particles. However, the precise molecular form and even the method of their incorporation into the aerosol particle is currently a subject of debate. Whether they are physically mixed

with the salts (*Ming and Russel*, 2001) or accumulate on the surface of the water surrounding the aerosol (*Ellison et al*, 1999) will affect the hygroscopic behavior of the aerosol particle, which in turn affects scattering and optical depth.

2. METHODOLOGY

Project RED employed two aerosol sampling platforms, one aboard the CIRPAS Twin Otter aircraft based out of Kaneohe Marine Corps Air Base on Oahu, and a second upon the FLIP (FLoating Instrument Platform) research vessel that was moored off the northeastern shore of Oahu. The Micro Orifice Uniform Deposit Impactor (MOUDI), as described by Gao et al (2002), was mounted on the wing of the Twin Otter and a 90 mm filter pak was employed upon the FLIP research vessel. The Twin Otter impactor also utilized blank filters that were stored under the same conditions as the exposed filters and used for subtraction of background aerosol loading during gravimetric and chemical analysis. To enhance the mass accumulation on the sample substrates, the MOUDI impactor had its intermediate stages removed and was used as a standard filter sampler (one substrate collected all sizes).

The filters were extracted using 10mL aliquots of HPLC grade water and underwent chemical analysis utilizing inductively coupled plasma atomic emission spectrography, ion chromatography and electrospray ionization-ion trap mass spectrometry. The procedure followed was identical to that described by Gao et al (2002). These techniques identified a total of 11 inorganic ions, 4 carboxylic acids and 2 carbohydrates.

Absorption and scattering data were gathered using three instruments aboard the Twin Otter aircraft: the University of Washington passive humidigraph (*Gasso et al*, 2000), the TSI nephelometer (*Anderson et al*, 1998) and the PSAP (*Bond et al*, 1999).

3. RESULTS

The results of the chemical analysis and the corresponding gamma values and 550nm scattering, corrected for instrument noise and angular truncation as specified by Anderson (1998), are given in Tables 1 and 2. The exact speciation of chemicals identified is given in the Principal Component Analysis.

Principal Component Analysis with Varimax Rotation, which maximizes the orthogonality of the eigenvectors, was performed on the data from FLIP. The variables were resolved into two components

^{*} *Corresponding Author:* Kathleen Crahan, Dept. Of Atmospheric Science, Box 351640, University of Washington, Seattle, Washington 98195-1640. Email: katie@atmos.washington.edu

Filter Number	Date Collected	Air Source	Altitude (ft)	550 nm Scatter (*10 ⁻⁶ m ⁻¹)	Gamma	Total Inorganic Concentration (ug/m ³)	Total Organic Concentration (ug/m ³)
TO04	8/24/01	Marine	100	8.872	0.456	2.476	0.322
TO05	8/24/01	Marine	400	8.770	0.719	6.750	0.000
TO10	8/28/01	Coastal-marine	100	22.593	.	1.872	0.000
TO11	8/28/01	Coastal-marine	100	18.980	0.443	2.561	0.019
TO12	8/28/01	Coastal-marine	600	17.776	0.476	1.132	0.391
TO13	8/28/01	Coastal-marine	600	19.037	0.454	1.836	0.127
TO15	8/29/01	Marine	100	18.635	0.383	2.281	0.000
TO18	8/29/01	Marine	600	16.379	0.436	3.562	0.000
TO19	8/30/01	Marine	100	19.152	0.551	2.253	0.009
TO20	8/30/01	Marine	100	19.511	0.375	2.119	0.015
TO21	8/30/01	Marine	600	19.030	0.460	2.962	0.021
TO26	9/4/01	Island	2000	4.965	0.215	1.243	0.134
TO90401 3C	9/4/01	Island	150	6.971	0.280	2.625	0.000
TO90401 4D	9/4/01	Island	2000	5.843	0.269	0.430	0.000
TO27	9/5/01	Island	150	5.978	0.157	1.164	0.010
TO28	9/5/01	Island	1850	4.345	0.137	0.000	0.017
TO90501 5E	9/5/01	Island	150	7.367	0.173	1.528	0.000
TO90501 6F	9/5/01	Island	1200	6.784	0.211	0.239	0.018
TO29	9/6/01	Island	150	5.982	0.284	0.252	0.005
TO31	9/6/01	Island	200	6.152	0.273	0.233	0.000
TO32	9/6/01	Island	2000	4.461	0.254	0.067	0.000
TO90601 4D	9/6/01	Island	2150	6.164	0.210	0.177	0.058
TO33	9/10/01	Island	150	18.751	0.320	1.994	0.000
TO34	9/10/01	Island	1650	15.133	0.314	1.408	0.024
TO37	9/14/01	Island	100	8.653	0.181	0.626	0.000
TO38	9/14/01	Island	1550	8.254	0.187	0.493	0.057

Table 1: Chemical Analysis Results for Twin Otter Filter Data.

as shown in Table 3. The first component suggests an air mass strongly influenced by land. Silicon, iron, and aluminum have dust sources in their oxide form common in volcanic and soil dust. Nitrate and non-sea salt sulfate show anthropogenic pollutants to be well mixed with the dust in the first component. The strong oxalate loading in the first component is not surprising considering it is a common breakdown product of many organic anthropogenic pollutants.

The second component shows a more obvious marine forcing with strong loadings of sodium and chloride, as well as calcium and magnesium, which are found in salt form in ocean water. Succinate also shows a strong correlation with the marine component. This is

in accord with previous studies that also noted the presence of succinic acid in marine air samples (*Kawamura et al, 1999*), marine cloud water samples (*Hegg et al, 2002*), and remote marine rain samples (*Semepere et al, 1995*). *Kawamura et al (1999)* proposed a formation mechanism of succinic acid through the photooxidation of unsaturated fatty acids commonly found in marine phytoplankton. The negative loading of glucose and levoglucosan on the two components suggests that the presence of the two carbohydrates lower the gamma values, as would be expected for hydrophobic compounds. Although the presence of glucose and levoglucosan may initially seem confusing, recent works (*Simoneit et al, 1998*,

Filter Number	Date Collected	Source	550 nm Scatter ($\times 10^{-6} \text{ m}^{-1}$)	Gamma	Total Inorganic Concentration ($\mu\text{g}/\text{m}^3$)	Total Organic Concentration ($\mu\text{g}/\text{m}^3$)
FP01	8/27/01	Marine	.	0.404	3.191	0.209
FP02	8/28/01	Coastal-marine	21.88	0.491	8.531	0.419
FP03	8/29/01	Marine	11.401	0.413	6.606	0.490
FP04	8/30/01	Marine	19.719	.	9.675	0.542
FP06	8/31/01	Marine	13.385	.	7.473	0.344
FP07	9/1/01	Island	.	.	7.050	0.402
FP08	9/2/01	Island	.	.	3.531	0.146
FP09	9/3/01	Island	.	.	3.072	0.219
FP10	9/4/01	Island	6.571	0.325	3.397	0.567
FP11	9/5/01	Island	6.436	0.175	4.168	0.297
FP12	9/6/01	Island	6.189	.	2.575	0.149
FP13	9/7/01	Island	.	.	3.560	0.134
FP14	9/8/01	Island	.	.	4.111	0.322
FP15	9/9/01	Island	.	.	3.992	0.129
FP16	9/10/01	Island	19.378	.	8.747	0.414
FP17	9/11/01	Island	.	.	4.102	0.142
FP18	9/12/01	Island	.	.	4.842	0.186
FP19	9/13/01	Island	.	.	5.704	0.184
FP20	9/14/01	Island	9.156	.	1.931	0.078

Table 2: Chemical Analysis Results for FLIP Filter Data.

Component	1	2
550nm SCATTERING	0.880	0.475
GAMMA	0.739	0.674
CALCIUM	0.576	0.817
IRON	0.871	0.492
POTASSIUM	0.316	0.949
MAGNESIUM	0.193	0.981
SODIUM	0.638	0.770
SILICON	0.984	0.180
ALUMINIUM	0.984	0.180
NITRATE	0.714	0.700
GLUTARATE	0.984	0.180
SUCCINATE	0.150	0.989
MALONATE	0.765	-0.644
SULFATE	0.867	0.499
OXALATE	0.967	0.255
PHOSPHATE	-0.287	0.958
NSS_SULFATE	0.910	0.415
CHLORIDE	0.399	0.917
LEVOGLUCOSAN	-0.503	-0.864
GLUCOSE	-0.998	0.070

Table 3: FLIP Chemical Composition Principal Component Analysis with Varimax Rotation.

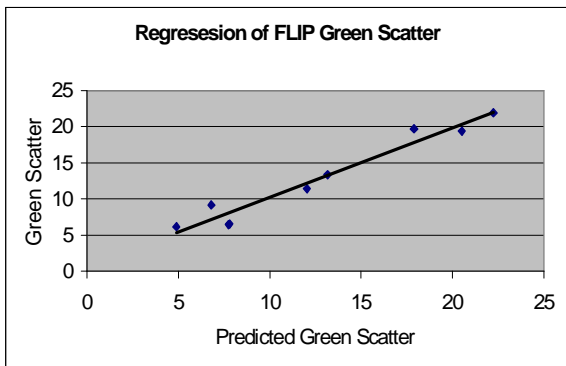


Figure 1: A Regression of Measured 550nm Green Scatter Values and Predicted Green Scatter Values Using Sodium and Oxalate as Sea Salt and Pollution Tracers, Respectively

Fraser *et al*, 2000) show that levoglucosan is emitted at high concentrations in biomass burning and, as it is stable for several days, it can be used as a long-range tracer for biomass burnings (a source for relatively hydrophobic aerosols). Satellite photos have revealed large burning areas on both the Big Island of Hawaii and in several spots on the West Coast of the United States during the field campaign.

Gamma values and corrected dry green scattering measured aboard the Twin Otter aircraft were collated with FLIP filters whenever possible. The lowest level passes of the Twin Otter near FLIP (~ 30m MSL) were assumed representative, with respect to aerosol hygroscopicity and light scattering, of data at the filter sampling location on FLIP (~15m MSL). The data were filtered to ensure that only cases in which gamma was essentially constant from pass to pass were utilized. This was done because the filter sampling intervals subsumed many Twin Otter passes and variations between gamma and composition could add noise to the data. Both gamma and 550nm scattering appear most strongly correlated with the land-influenced air mass, but do have significant loading on the marine component as well. To further explore this, multiple linear regression was performed on the chemical analysis results. The initial regression upon gamma produced negative coefficients for the sea salt component of the equation, which is non-physical, and the regressions were performed again with a constant of zero forced upon the results. The same analysis was performed on the green scatter values, and the results are seen in Figure 1 and Figure 2.

Using sodium as a tracer for the marine component and oxalate as a land-influenced air mass tracer, 70% of the gamma values were explained by the sea salt, and 22% by the pollution. The results of the regression are shown in Figure 2. To further test the robustness of the component contributions, the regression analysis was performed using other tracers such as chloride, sulfate, and nitrate. Averaging the values gives a sea salt gamma value contribution of 59

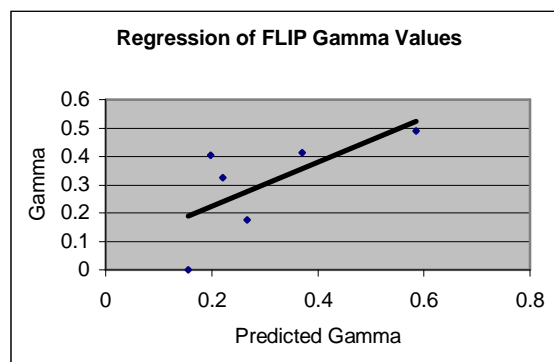


Figure 2: A Regression of Measured and Predicted Gamma Values Using Sodium and Oxalate as Sea Salt and Pollution Tracers, Respectively.

$\pm 20\%$ and a pollution contribution of $25 \pm 12\%$. This is in contrast to the PCA results, which placed a slightly heavier gamma weighting on the pollution component. However, as there are significant loadings on both components, the two results are not incongruous.

A better fit was obtained for the green scatter values, as seen in Figure 1. The various tracers utilized showed little variance, with an average sea salt contribution of $49 \pm 6\%$ to the corrected dry green scattering, and a pollution contribution of $36 \pm 8\%$.

Performing similar analyses on the Twin Otter filter results, the Principal Component Analysis revealed five factors, a much more complex situation. The first factor, heavily loaded with nitrate, sulfate, and NSS sulfate, represents the pollution component of the air mass. The marine air component revealed in the analysis is heavily loaded with sodium, chloride, and succinate, again strongly supporting Kawamura's proposal for succinic acid formation from marine fatty acids. Interestingly, levoglucosan continues to be most strongly associated with the land-influenced pollution factor, and oxalate has become more closely associated with the sea salt component. Kawamura *et al* (1999) did speculate on the production of small diacids during long-range atmospheric transport of organic marine aerosols, which would explain a stronger marine component of oxalate, a C2 diacid, at higher altitudes.

The third, fourth, and fifth components, containing potassium, phosphate, calcium, glucose, and silicon, are less easily explained. The robustness of the results was tested when the Principal Component Analysis was performed upon the Twin Otter data while forcing the results into four factors. The pollution and sea salt factors remained essentially unchanged, phosphate became more closely associated with the pollution component, and the silicon, calcium, glucose, and potassium loadings from the third, fourth and fifth component were forced onto two components.

Again examining the gamma values and 550nm scattering loadings, gamma and green scattering both seem to be most strongly associated

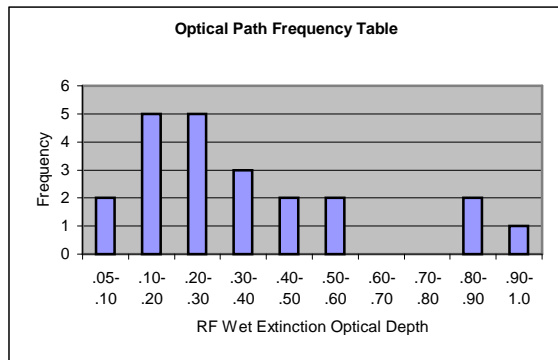


Figure 3: Frequency Distribution of Calculated Wet Extinction Optical Depths along the RF Signal Path.

with the pollution component. The scattering also has a high loading on the sea salt component but this is surprisingly not shared by gamma. Only weak associations with the remaining three factors are found for both scattering and gamma. The initial linear regression analyses for light scattering and gamma revealed a constant with a heavy weighting in the results, and as most of the gamma and scattering were explained by the first two eigenvectors in the Principal Component Analysis, the regression was performed again without a constant. The results revealed a sea salt gamma contribution of $36 \pm 12\%$ and a pollution contribution of $42 \pm 13\%$. The light scattering budget suggests, on average, a $43 \pm 10\%$ sea salt contribution and a $37 \pm 13\%$ pollution contribution. It is interesting to note that the relative contribution of sea salt to both the gamma values and scattering values decreased from the FLIP regression analysis to the Twin Otter regression analysis. This can be explained by the greater sea salt concentration found at lower altitudes near the surface of the ocean.

The optical depths along the RF signal propagation path, which ran between transmitters on FLIP and a shore receiver based in Kaneohe Marine Corps Air Base, and the EO signal propagation path between FLIP and Malaekahana State Park on Oahu were calculated using the corrected green light scattering values and corrected absorption values as specified in Bond et al (1999). Estimating mean scattering and absorption values along the path, then multiplying scattering at both dry and ambient humidities by the path length (approximately 26km and 10km for the RF and EO signal path, respectively), and finally multiplying the sum of the scattering (both wet and dry) and absorption by the path length will reveal the wet and dry scattering and extinction optical depth. The frequency distribution of the wet extinction optical depth along the RF path is shown in Figure 3.

A case study was performed on dates with three different air sources: marine air where backward trajectory calculations utilizing the HYSPLIT4 modeling routine (HYSPLIT4, 1997) traced the air mass traveling westward from the western US, marine coastal air that

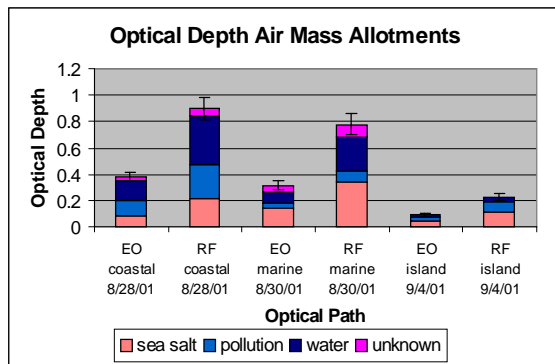


Figure 4: A Case Study of EO and RF Optical Paths Optical Depths.

traveled in a northwesterly direction skimming the coast of Maui and the Big Island, and island influenced air that traveled eastward across Oahu before arriving at the sampling venues. The contributions to green scattering were calculated from the linear regression analysis performed upon the Twin Otter data with chloride and sulfate used as the predictants and shown in Figure 4. The 550nm scattering was calculated using equation 2:

$$\sigma_{sp} = 8.798(\text{sulfate}) + 12.195(\text{chloride}) \quad (2)$$

The scattering due to water was derived by subtracting the ambient 550nm scatter from the dry 550nm scatter, and the contribution of unknown sources was calculated by subtracting the sum of the calculated scatter from the measured scatter. Within the six cases studied an average of 95% of the light scattered was attributable to the three sources. The higher scattering caused by sea salt for the flight on 8/30/01 could be caused by higher surface winds seen that day. The lower level of sea salt seen for the island air case is expected, but the corresponding low level of pollution is puzzling.

4. CONCLUSIONS

Analysis of the data collected during the Project RED experiment has demonstrated the strong link between chemical composition of aerosols and the hygroscopic and light scattering behavior of them. Using chemical predictors to approximate sea salt and pollution contribution to the gamma and scattering budgets of measurements near the sea surface, 84% and 85% of the budgets were accounted for, respectively. The different sources measured from the Twin Otter aircraft were not as easily categorized, but there were clear sea salt and pollution components. Linear regression results were averaged to show that 78% of the estimated hygroscopicity and 80% of the light scattering budget could be attributed to the two sources.

The role of organics has not been fully explored in the aerosol behaviors observed during the field campaign, but at the concentration level identified, they certainly must play a role. Possible further

analyses include closure studies with a detailed theoretical (composition based) model of aerosol hygroscopicity.

ACKNOWLEDGEMENTS

Support for this research was provided by ONR grant N00014-97-1-0132 and NSF grant ATM 9908471.

References

- Anderson, T. A. and J. A. Ogren, 1998: Determining aerosol radiative properties using the TSA 3563 integrating nephelometer. *Aerosol Sci. & Technol.*, **29**, 57-69.
- Bond, T.C., T. A. Anderson and D. Campbell, 1999: Calibration and intercomparison of filter-based measurements of visible light absorption by aerosols. *Aerosol Sci. & Technol.*, **30**, 582-600.
- Charlson, R. J., S. E. Schwartz, J.M. Hales, R. D. Cess, J. A. Coakley Jr., J. E. Hansen and D. J. Hoffmann, 1992: Climate forcing by anthropogenic aerosols. *Science*, **255**, 423-430.
- Ellison, G. B., A. F. Tuck and V. Vaida, 1999: Atmospheric processing of organic aerosols. *J. of Geophys. Res.*, **104**, 11,633-11,641.
- Fraser, M. P. and K. Lakshmanan, 2000: Using levoglucosan as a molecular marker for the long-range transport of biomass combustion aerosols. *Environ. Sci. Technol.*, **34**, 4560-4564.
- Gao, S., D. A. Hegg, P. V. Hobbs, T. W. Kirchstetter, B. J. Magi and M. Sadilek, 2002: Water soluble organic components in aerosols associated with savanna fires in southern Africa: identification, evolution, and distribution. *J. Geophys. Res.*, In Press.
- Gassó, S., D. A. Hegg, D. S. Covert, D. Collins, K. J. Noone, E. Ostron, B. Schmid, P. B. Russell, J. M. Livingston, P. A. Durkee and H. Jonsson, 2000: Influence of humidity on the aerosol scattering coefficient and its effect on the upwelling radiance during ACE-2. *Tellus*, **52B**, 546-567.
- Hegg, D. A., S. Gao and H. Jonsson, 2002: Measurements of selected dicarboxylic acids in marine cloud water. *Atmos. Res.*, **62**, 1-10.
- HYSPLIT4, 1997: Hybrid Single-Particle Lagrangian Integrated Trajectory Model. Web Address: <http://www.arl.noaa.gov/ready/hysplit4.html>, NOAA Air Resources Laboratory, Silver Springs, MD.
- IPCC, 2001: *Climate Change 2001, The Scientific Basis*. Cambridge University Press, Cambridge, UK, pp. 392-393.
- Kasten, F., 1969: Visibility forecast in the phase of pre-condensation. *Tellus*, **21**, 631-635.
- Kawamura, K., and F. Sakaguchi, 1999: Molecular distribution of water soluble dicarboxylic acids in marine aerosols over the Pacific Ocean including tropics. *J. Geophys. Res.*, **104**, 3501-3509.
- Ming, Y. and L. M. Russell, 2001: Predicted hygroscopic growth of sea salt aerosols. *J. Geophys. Res.*, **106**, 28, 259-28,274.
- Sempéré, R. and K. Kawamura, 1996: Low molecular weight carboxylic acids and related polar compounds in the remote marine rain samples collected from Western Pacific. *Atmos. Environ.*, **30**, 1609-1619.
- Simoneit, B. R. T., J. J. Schauer, C. G. Nolte, D. R. Oros, V. O. Elias, M. P. Fraser, W. F. Rogge, and G. R. Cass, 1999: Levoglucosan, a tracer for cellulose in biomass burning and atmospheric particles. *Atmos. Environ.*, **33**, 173-182.